Available online at www.sciencedirect.com

ScienceDirect

Procedia Materials Science 3 (2014) 1459 – 1466

Procedia Materials Science

www.elsevier.com/locate/procedia

20th European Conference on Fracture (ECF20)

On fatigue behaviour of two spring steels. Part II: Mathematical models

Donka Angelova, Rozina Yordanova, Svetla Yankova *

University of Chemical Technology and Metallurgy, St. Kliment Ohridski 8, Sofia 1756, Bulgaria

Abstract

Symmetric fatigue in two spring steels is investigated in three groups of specimens. One of the groups (Steel EN10270-1SH/ DIN 17223C – C 0.82%, Mn 0.76%, Si 0.26%) has experienced rotating-bending fatigue in air, and the other two groups (Steel BS250A53/ DIN 55Si7 – C 0.56%, Mn 0.81%, Si 1.85%), torsion fatigue in-air and corrosion environment. All experiments include testing to fracture, applying acetate-foil replication technique, replica monitoring of short crack surface growth, length measuring of propagating cracks, a, at the corresponding number of fatigue cycles, N. Data obtained from replica monitoring are presented in plots "Crack lengths, a – Cycles, N", and used for calculating fatigue crack growth rates, da/dN, and graphical presentations "Crack growth rates, da/dN – Crack lengths, a". A mathematical description of da/dN – a is presented by introducing a parabolic-linear model in different versions for each of the steels. The model versions are verified through comparing the experimental fatigue lifetimes with those calculated by the proposed model version.

Selection and peer-review under responsibility of the Norwegian University of Science and Technology (NTNU), Department of Structural Engineering

Keywords: rotating-bending fatigue, torsion fatigue, short fatigue-cracks, modeling of crack-growth rate, spring steel

1. Introduction

It is well known that fatigue life of technical components made of high-strength materials, and subjected to high-cycle fatigue, can be dominated up to 90% by stages of initiation and propagation of microstructurally short cracks. This supports the significance of quantitative analyses of all physical mechanisms being responsible for local stress

* Corresponding author. Tel.: +359 879 601 737.
E-mail address: donkaangelova@abv.bg

Selection and peer-review under responsibility of the Norwegian University of Science and Technology (NTNU), Department of Structural Engineering
doi:10.1016/j.mspro.2014.06.236

concentration, plastic deformation and, eventually, the initiation and propagation of short fatigue cracks which are very different from traditionally investigated long fatigue cracks Miller (1991), Suresh (1998). The early propagation mechanisms of short fatigue cracks are strongly related to the local microstructural features. Only when the sizes of these features become small than the crack length, predictions of crack propagation rates can be made on the basis of linear-elastic fracture mechanics. Fatigue long/short crack growth characteristics are normally expressed by the relation between crack growth rate and stress intensity factor range/short crack length, which involves two very different methods (by nature) for data obtaining based on different kind of specimens when observing and registering different physical cracks - long cracks, and physically small and short cracks Suresh (1998), Krupp (2007); also the two methods concerning long and short cracks use different technical standards Dowling (2006).

2. Experimental work

2.1. Material and specimens. Testing.

In the present study, fatigue in two spring steels are investigated: (i) Steel EN10270-1SH/ DIN 17223C (Steel A) for conducting own fatigue experiments, Angelova et al. (2013), (2014), and proposing new mathematical models of short fatigue crack growth; and (ii) BS250A53/DIN 55Si7 (Steel B) for using some already published results, Murtaza (1992), describing those results by the newly-proposed mathematical models of short fatigue crack growth, and making comparative analysis with Steel A. The microstructure, chemical compositions and slightly different hour-glass shape of specimens of Steel A and Steel B are presented in Angelova et al. (2014), Murtaza (1992).

Steel A. Twelve hourglass-shaped specimens were subjected to symmetric cyclic rotating-bending fatigue (RBF) at different stress ranges (Ду = 800, 1000, 1200, 1400, 1500 MPa), frequency of f=11 Hz and air environment.

Steel B. Fourteen hourglass-shaped specimens were exposed to fully reversed torsion fatigue (TF), and frequency f=5 Hz for two sets of stress ranges Дф = (915, 1080, 1106 MPa in air), (404, 601, 815, 900 MPa in corrosion).

For both steels a traditional replication technique was used; all details are given in Angelova et al. (2014).

2.2. Fatigue crack growth modelling.

Since the beginning of the last two decades it has been well established that the fatigue behaviour of metals can be described by three distinct regimes - microstructurally short cracks (MSC), physically small cracks (PSC) and long cracks (LC). Each type of crack requires different analytical approach characterizing its behaviour, i.e. microstructural fracture mechanics (MFM), elastic-plastic fracture mechanics (EPFM) and linear elastic fracture mechanics (LEFM), respectively. In terms of driving stresses there exist two basically different forms of crack, a Stage I crack developed by shear stresses, and a Stage II crack developed by tensile stresses. The limits of the transition zone between a propagating Stage I shear crack and a continuously growing Stage II tensile crack (the PSC zone) are emphasized by Miller (1993a) as two fundamentally different threshold conditions (or barriers d_1 and d_2) representing a "microstructural-dependant state" and "mechaniical stress-strain-dependant state". The barrier d_1 is defined by short fatigue crack experiment and d_2 - by long fatigue crack experiment using the same material.

Based upon the experimental data for short fatigue crack behaviour there are a few basic models describing it, the most known of which are those of Hobson and Brown (1986) - H-B and Akid and Murtaza (1995) - A-M, which present crack growth rate as a combined parabolic (Stage I of MSC) and linear (Stage II of PSC and LC) functions of crack length. The H-B model (for symmetrical push-pull fatigue) consist of one parabola and one line, considering one barrier of type d_1 and one, d_2. The A-M model (for TF) includes four barriers of type d_1 and one of type d_2 for in-air fatigue; and two barriers d_1 and one d_2 for corrosion fatigue. The H-B and A-M models are revised by Angelova (1998) - becoming H-B-A and A-M-A - who introduces a special modelling of PSC zone between a Stage I shear crack and a Stage II tensile crack. In this way two important tasks were solved: a more precise description of PSC behaviour; and finding the barrier of type d_2 from the same short fatigue crack experiment.

The complicated defining of the barriers d_1 and d_2, and the parabolic functions in H-B-A and A-M-A models was replaced with simplified methodic by Yordanova (2003), which is more convenient for practical use and a quick (express) evaluation of fatigue at keeping the basic concept for separated description of MSC (parabolic function), PSC (parabolic function) and LC (linear function) and conducting only short fatigue crack experiment.

The new model is presented in Eq.1:

$$\mathbf{M(a):}\begin{cases} MSC: (da/dN)_{ms} = D_1 a^2 + D_2 a + D_3;\ a \in [a_0,\ d_1];\ N_I; \rightarrow \\ PSC: (da/dN)_{ps} = D_4 a^2 + D_5 a + D_6;\ a \in [d_1,\ d_2];\ N_{II}; \rightarrow \\ LC: (da/dN)_l = D_7 a^{D_8};\ a \geq d_2;\ N_{III} \end{cases} \quad (1)$$

where: $(da/dN)_{n+1} = (a_{n+1} - a_n)/(N_{n+1} - N_n)$ is the crack growth rate *da/dN*; D_i, i=1-8 – materials constants; N_I, N_{II}, N_{III} – the corresponding number of cycles to crack regimes, MSC, PSC, LS; d_1 and d_2 – the microstructural barriers analytically determined after Yordanova's methodic, described in detail in Yordanova (2003).

This model is supported by the comparison of the fatigue lifetime predicted by Eq. (2), $N_{f,m}$, and the actual fatigue lifetime, $N_{f,\exp}$: $N_{f,m} = N_{f0} + N_I + N_{II} + N_{III}$ or in more detail, Yordanova (2003):

$$N_{f,m} = N_{f0} + \int_{a_0}^{d_1} 1/(da/dN)_{ms}\, da + \int_{d_1}^{d_2} 1/(da/dN)_{ps}\, da + \int_{d_2}^{a_f} 1/(da/dN)_l\, da, \quad (2)$$

where N_{f0} is the number of cycles to crack initiation, a_0 – the initial crack length and a_f – the final crack length.

The following formulae $(N_{f,m} - N_{f,\exp})100/N_{f,\exp}$, % is used as an evaluation of the adequacy of the proposed new model and if its value is in the error band $\pm$ 25 %, the mathematical description is accepted as adequate.

3. Results and discussion

Data obtained for Steel A and published for Steel B - *a* and N - are presented in Figs. 1a, b,c respectively, and dependences "Crack length, *a* – Numbers of cycles, *N*", "*a*–*N*", plotted in the same figures. The Steel A curves "*a*–*N*" for RBF, Fig.1a, show that both major cracks (for $\Delta\sigma$ = 1200 and 1400 MPa) have originated first. It can be seen that the major crack in the family "Major crack - Secondary cracks", "MC-SC", at $\Delta\sigma$ = 1400 MPa has initiated in an earlier stage in comparison with the initiation stages of all secondary cracks. At the same time the major crack and the secondary cracks in the family "MC-SC" at $\Delta\sigma$ = 1200 MPa show small difference at the number of cycles to initiation, close propagation (in terms of cycles) and a kind of competition between the secondary cracks for merging their propagation paths with that of the major crack. The surface of whole working area shows (by observation after specimen's fracture) unusual roughness, probably due to specimen polishing Angelova et al. (2013), (2014), confirming the strong influence of the surface-condition factor on fatigue behaviour. The curves "*a*–*N*" for Steel B (TF) are plotted in Fig. 1b,c. They show a major crack and only a few secondary cracks in each family "MC-SC" corresponding to a given stress range. An exception is the family "MC-SC" at $\Delta\tau$ = 900 MPa in corrosion with several secondary cracks. The family "MC-SC" at $\Delta\tau$ = 817 MPa in corrosion has more secondary cracks than those at $\Delta\tau$ = 404 and 601 MPa. Then the two families "MC-SC" at $\Delta\tau$ = 817 and 900 MPa having more secondary cracks are located very closely (in terms of cycles), which shows that above $\Delta\tau$ = 817 MPa the surface short cracks propagation and paths look like those of the family "MC-SC" of Steel A at $\Delta\sigma$ = 1200 MPa. This means that nature of material is of great importance, but varying with fatigue loading and kind of scheme, environment and surface condition, it is possible to observe a similar short fatigue crack behaviour of different materials.

An interesting fact can be mentioned. During the transition regime of PSC some specific events take place: **(i)** As a crack grows longer at a constant cyclic stress range, its plastic zone size controlling crack growth rate, increases.

However, the actual onset and extent of crack tip plasticity are functions of the cyclic stress-strain curve, and its well known that normally materials having a high yield strength and exhibiting cyclic strain hardening behaviour have a small plastic zone size at crack tip, and smaller crack growth rate compared with a lower yield strength materials that cyclically soften - originally mentioned by Miller (1993b). It has been shown that for a cyclic hardening material, the hardening rate is lower than the critical value which renders a continuously increasing plastic zone size relative to crack length - discussed for the first time by Navarro et al. (1992). **(ii)** During the PSC

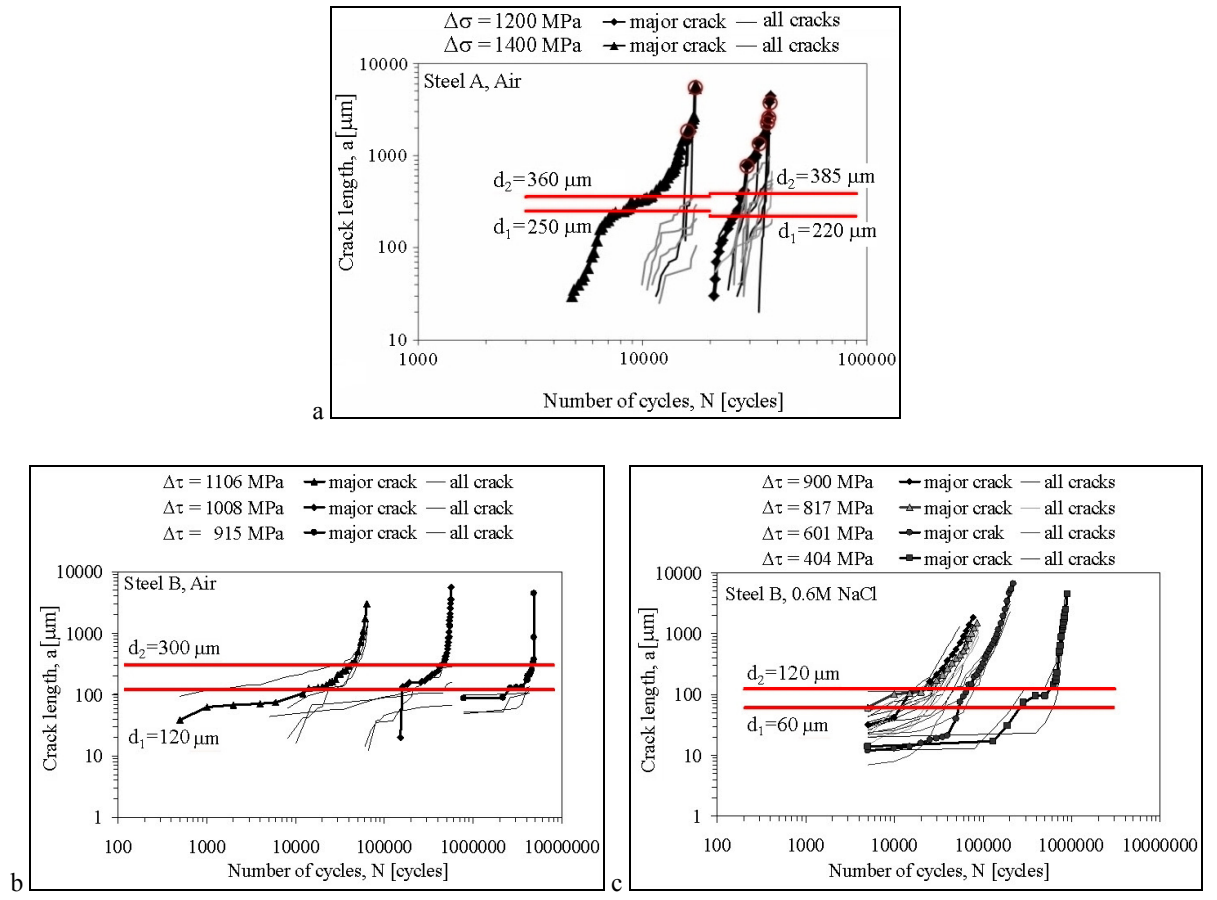

Fig. 1. Plots "Crack length, *a* – Numbers of cycles, *N*" and lines d_1 and d_2 defining PSC regime for Steels: (a) A - RBF; (b) & (c) B – TF

regime, microstructural barriers between grains are located in both tangential and normal directions to the advancing crack front. As the crack advances past the first dominant structural barrier it will still be decelerating as it approaches subsequent barriers, but to a lesser extent, before finally accelerating as it escapes the influence of barriers at a > d_2.

In addition to that, at some conditions as increased stress range, rough surface, aggressive environment, the cyclic plastic behaviour of materials can be exhausted quickly, in fact there is not time enough for plasticity realization.

The cases of PSC regimes of Steel A at Δσ = 1200 MPa and Steel B at Δτ = 817 MPa and 900 MPa can be treated in the above mentioned way. Steels A and B show a high yield strength and appearance of many secondary cracks initiating in narrow cycle interval in MSC regime (Stage I) of the major crack. Later on these secondary cracks probably help with plasticity exhaustion in PSC regime - Stage II (described by EPFM), influencing the behaviour of the major crack, Figs. 1a, b, c. After the plasticity exhaustion and still in PSC regime, the major crack transforms from shear mode into tensile mode; also do the secondary cracks. (In Figs. 1a, b, c the PSC regime is defined by lines showing barriers d_1 and d_2.) In LC regime (Stage II) some of the secondary cracks merge with the major crack.

Crack growth rates *da/dN* are calculated and presented versus crack lengths *a* for Steel A in Figs. 2, 3a, and for Steel B, in Fig. 4. Applying the Parabolic-linear model, PLM, of Yordanova (2003), Eq.1, to these data leads to obtaining of dependences "Crack growth rate, *da/dN* – crack length *a*". For Steel A the values of coefficients *D* are shown in Table 1, and the values of all the other fatigue characteristics, in Table 2.

Steel A. The graphical presentation of the applied PLM from Eq. 1 to the experimental data at Δσ = 1400 MPa can be seen in Fig. 2a. In this case the basic model is applied only to the major crack and is marked as version L of

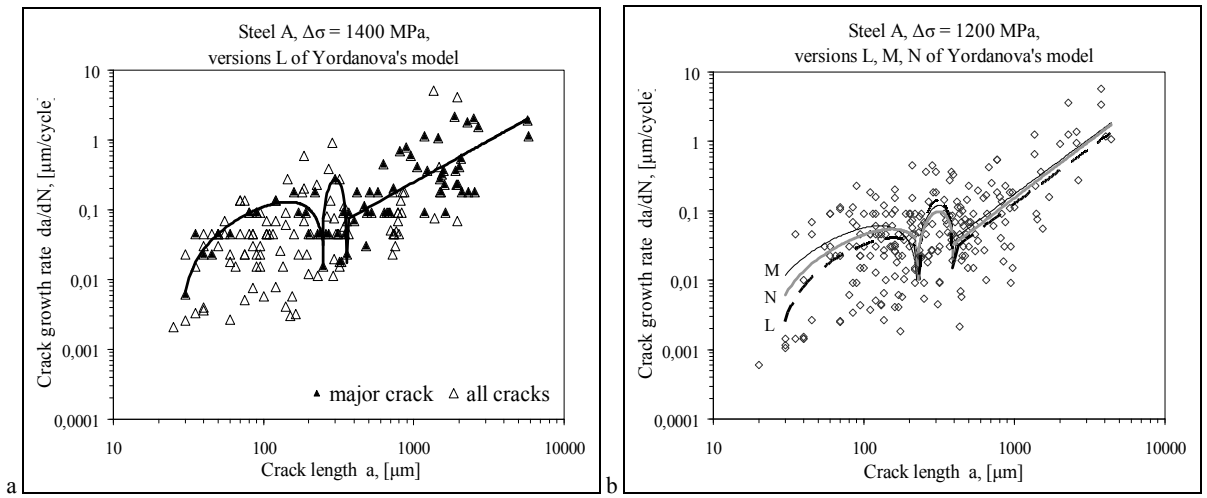

Fig. 2. New Parabolic-linear model "Crack growth rate, *da/dN* – crack length *a*" for Steel A: (a) L version, Δσ=1400 MPa;.(b) comparison between L, M and N versions, Δσ = 1200 MPa

it. The secondary cracks have not been taken into consideration. At the same time the graphical presentation of the applied PLM from Eq. 1 to the experimental data at Δσ = 1200 MPa is shown in Fig. 2b in three versions, and is very different from that in Fig. 2a. The version L presents crack growth rate only of the major crack. The version M shows a different behaviour of the major crack while influenced by the secondary cracks merging with it. The version N presents the major crack propagation involving all the secondary cracks. The three versions L, M and N are analytically described by Eq. 1 and Tables 1, 2. It is important to mention that for modeling different stages of the major crack propagation (MSC, PSC, LC), there are used only those data *da/dN, a* of the secondary cracks initiated or developed in the corresponding regimes of the major crack growth.

The comparison between the three versions (L, M, N) of the basic PLM at 1200 MPa (curves L, M and N), shown in Fig. 2b, can be used for usefulinteresting discussions. The curve M shows acceleration of crack growth rates for MSC and LC regimes in comparison with L and N curves, due to interaction and merge of the secondary cracks with the major crack. However in PSC regime the curve M is located below the curve L although very close to it. It is connected with the multitude of secondary cracks initiated easily due to the observed surface roughness and helping with plasticity exhaustion of Steel A in PSC regime of the major crack; also it is connected with the specific events taking part in PSC and described in *3.3. Transition regime PSC for Steels A and B*. So, we can conclude that at 1200 MPa, the version M of the basic PLM most realistically represents the fatigue behaviour of Steel A. At 1400 MPa there are registered only a couple of secondary cracks which merge with the major crack, Figs. 1a, 2a; their influence is exerted during the third stage (LC) and practically does not affect the major crack growth behaviour; in this case the version L of PLM takes place. The versions L, M, N at Δσ = 1200 MPa and version L at Δσ = 1400 MPa are shown together in Fig. 3a. The highest crack growth rates correspond to the highest stress range. At the same time the final length of the major crack at Δσ = 1200 MPa is 75% from the length of the major crack at Δσ = 1400 MPa. This can be explained as a result of both, a full and quick consumption of specimen plasticity at Δσ = 1200 MPa and a high degree of energy dissipation, due to initiation and development of many and more secondary cracks at that stress range, interacting and merging with the major crack.

Steel B. The graphical presentation of the applied PLM from Eq. 1 to the experimental data of Steel B (subjected to TF in-air and corrosion environment) can be seen in Fig. 4, and the version M of PLM is shown by thick line. The original model of Murtaza (having 4/2 microstructural barriers of type d_1 characterizing TF for in-air/corrosion environment, and one of type d_2) is plotted by dashed line in Fig. 4, too. In fact at corrosion condition *da/dN* increases, Figs. 4b, c; also the higher stress range plays the same role, leading to higher *da/dN*.

As illustrated in Figs. 2b, 3a, 4, a reasonable agreement can be seen when comparing experimental *da/dN* and theoretical ones using the new analytical model M described by Eq. 1 and Tables 1, 2 (the case when many

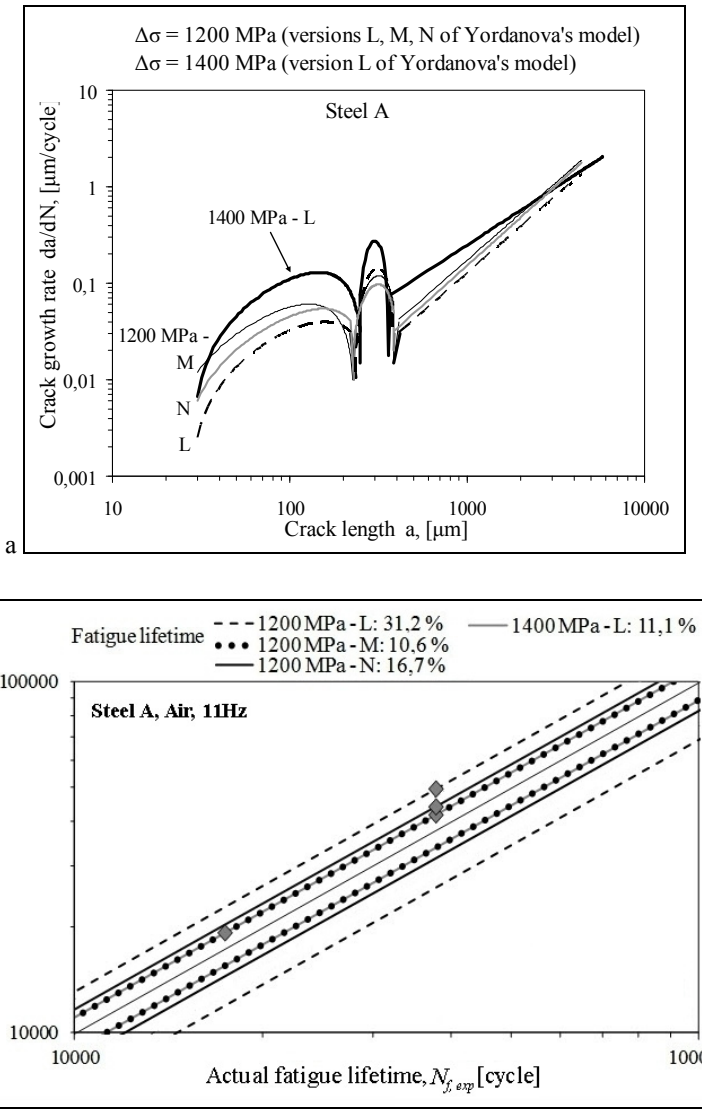

Fig. 3. Steel A tested at Δσ = 1200 MPa (L, M and N versions) and Δσ =1400 MPa (L version): (a) Comparison between the new parabolic-linear model; (b) Comparison between experimental and predicted fatigue lifetimes and the corresponding error bands in percentages.

Table 1. Values of coefficients D in Eq. 1 at Δσ = 1200 & 1400 MPa, Steel A.

Stage	D	1200 MPa			1400MPa
		L version	M version	N version	L version
1	2	3	4	5	6
MSC	D_1	-2,3E-06	-5,1E-06	-3,2E-06	-9,1E-06
	D_2	7,3E-04	1,3E-03	9,7E-04	2,7E-03
	D_3	-1,7E-02	-2,3E-02	-2,0E-02	-6,5E-02

1	2	3	4	5	6
PSC	D_4	-2,2E-05	-1,3E-05	-9,9E-06	-7, 5E-05
	D_5	1,4E-02	8,5E-03	6,2E-03	4,5E-02
	D_6	-2,0E+0	-1,2E+0	-8,8E-01	-6,5E+00
LC	D_7	2,0E-06	2,7E-06	1,7E-06	6,5E-05
	D_8	1,6E+00	1,6E+0	1,7E+00	1,2E+00

Table 2. Fatigue characteristics of Steel A for MSC, PSC, LC growth and some numbers of cycles during specimen fatigue lifetime.

Δσ, MPa		a_0, μm	d_1, μm	d_2, μm	a_f, μm	N_0, cycles	$N_{f,exp}$, cycles	$N_{f,m}$, cycles	$(N_{f,m} - N_{f,exp})100/N_{f,exp}$, %
1200	L version	30	220	385	4395	20790	37840	49654	31.,2
	M version							41867	10.6
	N version							44149	16.7
1400	L version	30	250	360	5835	4840	17380	19310	11.1

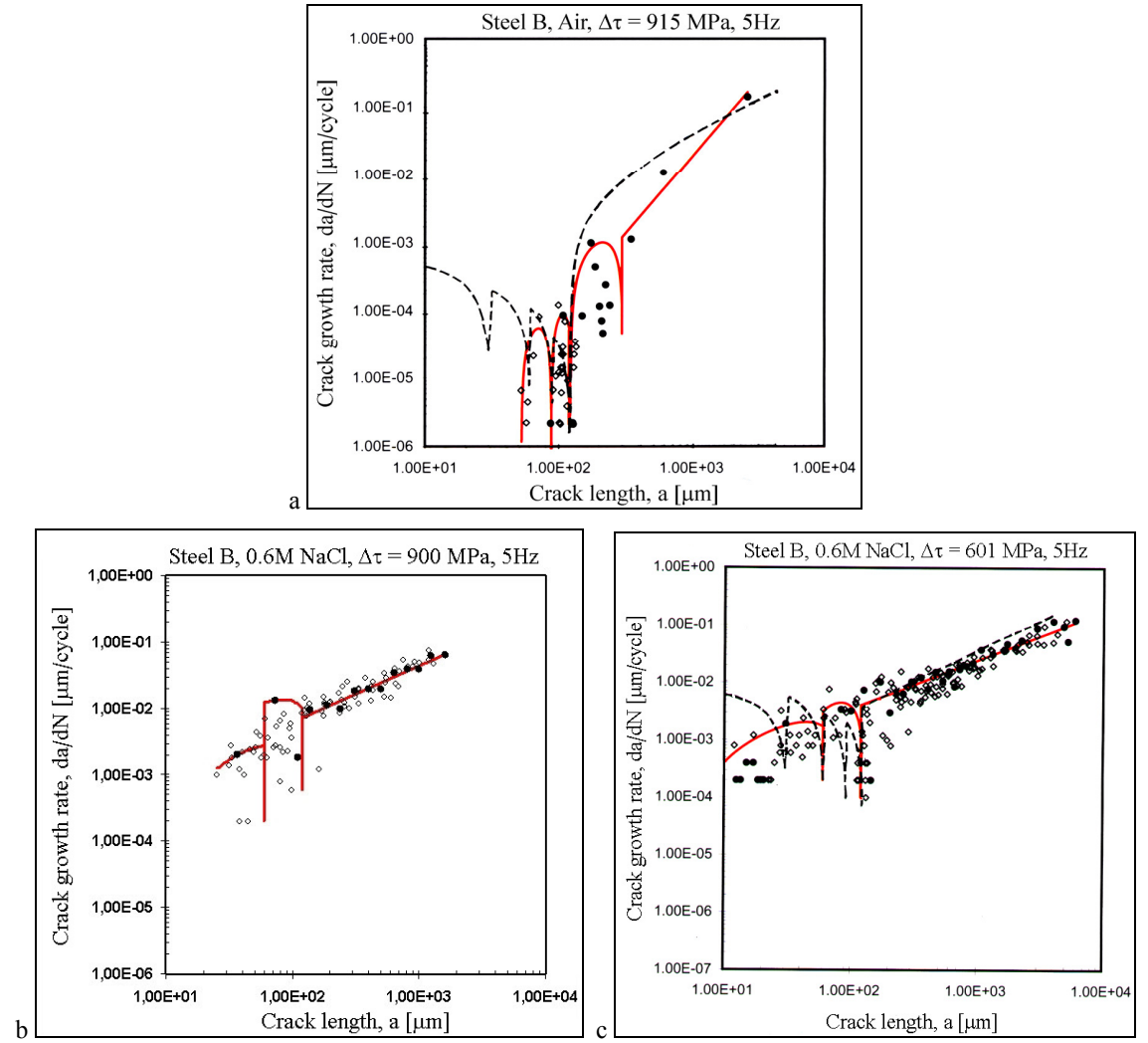

Fig. 4. Fatigue crack growth curves for Steel B: (a) air; (b), (c) corrosion.

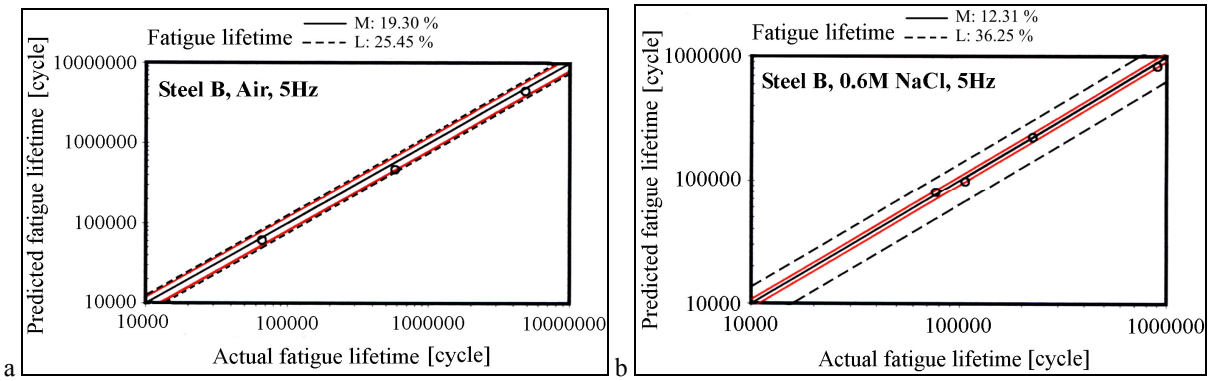

Fig. 5. Comparison between experimental and predicted lifetimes for Steel B with the error bands in percentages: (a) in air; (b) in corrosion.

secondary cracks have initiated and influenced the growth of major crack). The proposed new model M is supported by the comparison of predicted $N_{f,m}$, Eq. 2, and actual $N_{f,exp}$ fatigue lifetimes presented in Figs. 3b and 5.

4. Conclusions

Short fatigue crack behavior of two spring steels was investigated and analytically modeled: Steel EN10270-1SH/ DIN 17223C (Steel A) for own fatigue experiment; and BS250A53/DIN 55Si7 (Steel B) with already published fatigue data and for comparison with Steel A. Steel A is subjected to symmetric rotating bending fatigue in air, and Steel B - to fully reversed torsion fatigue in air and in corrosion environment.

For Steel A two cases of loading are discussed, $\Delta\sigma$ = 1200 MPa and $\Delta\sigma$ = 1400 MPa. In both cases the major surface crack originates first and develops in three regimes of propagation: MSC, PSC, LC. The major crack at $\Delta\sigma$ = 1400 MPa has initiated in an earlier stage than the secondary cracks and is well separated from them; it merges with only a couple of secondary cracks. At the same time the major crack at $\Delta\sigma$ = 1200 MPa propagates at condition of interaction between and with many secondary cracks in its vicinity at no big difference between their initiation stages; it leads to exhaustion of local plasticity in PSC regime, crack merging (six secondary cracks merge with the major crack) and complete failure. For Steel B some fatigue tests data of major and secondary cracks propagation are studied in-air and corrosion environment, considering specific features of the three regimes of major crack growth: MSC, PSC, LC.

For both steels short fatigue crack growth behaviour is modeled on the base of Hobson-Brown-Angelova, Akid-Murtaza-Angelova and Yordanova models. Three new versions of Yordanova model are proposed and approved at different conditions of loading, environment and specimen surface state; a special attention has been given to PSC regime of major crack propagation. The three proposed model versions are additionally supported by the comparison between the predicted and actual fatigue lifetimes.

References

Angelova D., Akid R., 1998. A Note on Modelling Short Fatigue Crack Growth Behaviour, Fatigue & Fracture of Engineering Materials & Structures, 21, 771-779.

Angelova D., Yordanova R., Nikolova L., Yankova Sv., 2013. Investigation on fatigue Behavior and Fatigue crack Growth of a Spring Steel. Part II: Mathematical description an Analyses, Scientific Proceedings, Year XXI, 2(139), 244-248.

Angelova D., Yordanova R., Lazarova Ts., YankovaSv, 2014. On fatigue behavior of two spring steels. Part I: Wöhler curves and fractured surfaces, 20th European Conference on Fracture, 30th June – 04th July, 2014, Trondheim, Norway.

Dowling N., 2006. *Mechanical Behaviour of Materials*, Prentice-Hall, New Jersey, USA.

Hobson P., Brown M., de los Rios E., 1986. Short fatigue cracks. In: EGP Publication 1, Mechanical Engineering Publications, London, 441-459.

Krupp U., 2007. Fatigue Crack Propagation in Metals and Alloys, Wiley-VCH GmbH and co. KGaA.

Miller K. J., 1991. Metal Fatigue – Past, Current and Future. Proc. Inst. Mech. Engrs, London.

Miller K. J., 1993-a. The two threshold of fatigue behaviour. Fatigue Fract. Engng Mater. Struct., 16, 931-939.

Miller K. J, 1993-b. Materials science perspective of metal fatigue resistance. Mater.Sci. Tech. 9, 453-462.

Murtaza G., 1992. Corrosion Fatigue Short Crack Growth Behaviour in a High Strength Steel. PhD thesis-University of Sheffield.

Murtaza G., Akid R., 1995. Modelling short fatigue crack growth in a heat- treated low alloy steel. Int. J. Fatigue 17, 207-214.

Navarro A., de los Rios E., 1992. Fatigue crack growth modelling by successive blocking of doslocations. Proc R. Soc. Lond. A 437, 375-390.

Suresh S., 1998. Fatigue of Materials. Cambridge Univ. Press, Cambridge, UK.

Yordanova R., 2003. Modeling of fracture process in low-carbon 09Mn2 steel on the bases of short fatigue crack growth experiments. Comparative analyses on the fatigue behavior of other steels, PhD Thesis, University of Chemical Technology and Metallurgy, Bulgaria.